Defence Research and Development Canada
Recherche et développement pour la défense Canada

DEFENCE R&D DÉFENSE

A new technique for separation of temperature and emissivity

Thermal infrared remote sensing

P. Lahaie
DRDC Valcartier

Defence R&D Canada – Valcartier
Technical Memorandum
DRDC Valcartier TM 2004-124
December 2004

Canada

A new technique for separation of temperature and emissivity

Thermal infrared remote sensing

Pierre Lahaie
DRDC Valcartier

Defense R&D Canada - Valcartier

Technical memorandum

DRDC Valcartier TM 2004-124

December 2004

Author

Pierre Lahaie

Approved by

J-M. Garneau
Section Head

Approved for release by

G. Berubé
Chief Scientist

Abstract

We describe in this report a new technique for the separation of temperature and emissivity in the thermal infrared part of the electromagnetic spectrum. The measurement taken with by a passive remote sensing instrument is radiance. This radiance is a combination of components originating from the atmosphere and from the ground. Once the atmospheric contribution is removed, the result is radiance from the ground that depends on its fundamental parameters i.e. temperature and emissivity. These parameters are useful to determine the nature and use of the material under observation. The new technique presented here is based on an iterative scheme for the selection of temperature and of its corresponding emissivity. At each temperature it evaluates a criterion, the total square error. The selected temperature is the one showing the smallest error. To evaluate the error we first compute the equivalent emissivity at a given temperature, we smooth the emissivity using a linear procedure then we compute a new radiance for the smoothed emissivity. The error is computed by the summation of the squared difference between the ground radiance and the new radiance. This technique is robust to noise and atmospheric parameters errors. The currently airborne imaging FTIR sensor (AIRIS) built by DRDC Valcartier is targeted as an application of interest for this algorithm. However, it can be applied to imaging sensor with at least six bands.

Résumé

Nous décrivons dans ce rapport une nouvelle technique destinée à permettre la séparation de la température et de l'émissivité dans la gamme infrarouge thermique du spectre électromagnétique. Les mesures obtenues par l'entremise d'un capteur passif en télédétection sont une combinaison de la contribution provenant de l'atmosphère et du sol. La contribution atmosphérique éliminée, on obtient seule une radiance provenant du sol. Cette dernière dépend de paramètres fondamentaux du sol; la température et l'émissivité. Ces derniers sont utiles pour l'identification de la nature et de l'utilisation des matériaux sous observation. La technique présentée ici s'appuie sur une estimation itérative de la température et de l'émissivité qui lui correspond. Pour chaque valeur de température, on estime un paramètre d'erreur. La plus faible valeur de ce paramètre caractérise la température à sélectionner. L'evaluation de l'erreur est faite en estimant pour chaque valeur de température une émissivité correspondante. Cette émissivité est lissée au moyen d'une procédure linéaire. Nous calculons ensuite la radiance correspondant à cette émissivité. L'erreur est enfin calculée en faisant la somme des carrés de la différence entre la radiance émanant du sol et la radiance calculée. La technique est robuste au bruit d'instrumentation et résistante aux erreurs d'estimation des paramètres atmosphériques. Nous destinons l'application de notre technique au futur imageur FTIR qui est construit par RDDC Valcartier. Cependant la technique est applicable à beaucoup d'autre capteurs fonctionnant dans la gamme infrarouge thermique. Il suffit pour ces capteurs de posséder au moins six canaux de mesure.

This page intentionally left blank.

Executive summary

Hyperspectral imagery applications generate large hopes, especially in the thermal band that extends from 8 to 12 microns. These applications vary from target detection and identification to terrain characterization. The main source of signal is the material composing the pixel footprint. The fundamental properties of the material, emissivity and temperature, are responsible for the signal generation, while the atmosphere contributes to some signal modifications and generation. The emissivity is characteristic of the object nature and the temperature yielding its activity and its interaction with the environment.

The processing of thermal hyperspectral images includes the following steps: radiometric calibration, atmospheric contribution elimination, and the extraction of the fundamental parameters of the targets. This last step is in the thermal band the separation of temperature and emissivity. This document addresses only temperature and emissivity separation, for which a first version algorithm was designed and its behaviour under various operation conditions. The performance study of the algorithm is conducted only with simulations because at this time, there is not enough high quality data to carry out this work correctly.

The described algorithm possesses multiple strengths. It is resistant to noise; it generates results even when there is erroneous radiometric calibration of the data; it is also able to work when there are large errors in the atmospheric optical parameters; there is no bias introduced by random noise in the temperature estimation. Finally, it is able to work when the target emissivity is low. All these strengths constitute major improvements to similar published algorithms. However, it possesses difficulty when the emissivity of the target has large variations within the sensor spectral band. For these variable emissivities, the algorithm behaviour will be enhanced in its future versions.

The work performed in temperature and emissivity separation is one of the steps leading to a tool suite designed for processing thermal hyperspectral images with only in-scene information. This capability will make the image processing and extraction of all the information contained in an image independent of any other information sources. The work has been carried out in DRDC Valcartier under WBE 15ev11

Lahaie Pierre. 2004. A new technique for separation of temperature and emissivity. DRDC Valcartier TM 2004-124

Sommaire

Les applications de l'imagerie hyperspectrale suscitent de grands espoirs, en particulier dans la gamme thermique, celle des longueurs d'ondes comprises entre 8 et 12 microns. Ces applications vont de la détection et de l'identification de cibles, jusqu'à la caractérisation de terrain. La plus grande partie du rayonnement perçu par un capteur dans cette gamme provient de l'émission propre des objets sous observation. Les autres composantes du rayonnement sont générées par l'atmosphère. L'émissivité et la température sont les paramètres fondamentaux qui déterminent la quantité d'énergie émise par la cible. L'émissivité étant caractéristique de la nature de la cible et la température rendant compte de son activité et de son interaction avec l'environnement.

La chaîne de traitement des images hyperspectrales comprend: l'étalonnage radiométrique des données brutes fournies par le capteur, l'élimination de la contribution de l'atmosphère ou compensation atmosphérique, et enfin, l'extraction des paramètres fondamentaux des objets sous observation en réalisant la séparation de la température et de l'émissivité. Ce document traite seulement de la séparation de la température et de l'émissivité pour laquelle nous avons élaboré un algorithme dont nous décrivons la première version ainsi qu'une étude de comportement face à diverses conditions d'utilisation. La caractérisation du comportement est faite par simulation car nous manquons de données de qualité suffisante pour effectuer ce travail.

L'algorithme obtenu dans ce travail possède plusieurs forces; il est très résistant au bruit, il fonctionne lorsque l'étalonnage radiométrique du capteur est déficient et lorsque les paramètres optiques de l'atmosphère sont mal connus. Aucun biais n'est introduit dans l'estimation de la température par le bruit du capteur. Enfin, il est capable de travailler lorsque les émissivités sont faibles. Il s'agit ici d'améliorations importantes comparativement à divers algorithmes de même nature obtenus dans la littérature scientifique. Il possède cependant des difficultés lorsque l'émissivité de la cible varie fortement. L'amélioration du comportement dans ce cas fera l'objet d'une étude subséquente.

Le travail réalisé ici s'inscrit dans une démarche qui devrait permettre d'obtenir une suite d'outils qui traiterait les images hyperperspectrales thermiques en utilisant seulement les informations disponibles dans ces images. Cette capacité opérationelle rendra le sytème de traitement des images autonome pour l'extraction des informations de toute nature disponibles à l'intérieur des images. Le travail décrit dans ce rapport a été entièrement réalisé à RDDC Valcartier dans le cadre du projet 15ev11

Lahaie Pierre. 2004 A new technique for separation of temperature and emissivity.
DRDC Valcartier TM 2004-124

Table of contents

List of figures

Acknowledgements

The author wants to gratefully acknowledge J.P.Ardouin for his help during the research and the work done during the writing of this report.

1. Introduction

In relation with the design of a new hyperspectral airborne sensor, AIRIS based on FTIR imaging technology and operating in the thermal infrared DRDC Valcartier undertook work to develop an algorithm for temperature and emissivity separation in the thermal infrared band from 800 to 1250 cm^{-1}. This band is also known as LWIR for long wave infrared.

Current algorithms have been studied prior to the design of our technique. The techniques can be separated into two classes. The first class considers that radiation comes mainly from the ground so they completely ignore the incident radiation from the atmosphere and do not make use of the reference the atmosphere provides. This first class of algorithms generally produces an estimation of temperature corresponding to the highest brightness temperature of the sample at the wavenumber where the emissivity is the largest. At this point the emissivity is set to 1 or any given number lower than 1 and all other emissivities are computed relatively to that emissivity. We did not consider these techniques because we are interested in more precision for the estimation of temperature and emissivity. The second class of algorithm makes use of the available knowledge about atmospheric downwelling irradiance. The atmospheric downwelling radiation shows characteristics enabling the positioning of the maximum emissivity at an arbitrary value selected by an algorithm. This cannot be done if atmospheric radiation is ignored. Examples of such algorithms are the ASTER TES algorithm designed by Gillespie et al. [2], [3], [4] and of Borel's iterative spectral smoothness (ISSTES) [5], [6] method.

Gillespie technique was designed for application to data obtained from the ASTER multispectral sensor. It is however easily applicable to hyperspectral data with some minor modifications. The algorithm uses some a priori assumptions about the maximum of the emissivity to compute an initial value for the temperature and the emissivity. It then uses an estimation of the minimum emissivity and computes temperature and emissivity according to this minimum value. This algorithm is fast. On the other hand, the ISSTES technique is different. It iteratively tries different temperature and chooses the right one according to a smoothness criterion. The criterion is computed as the variance of the output of a digital linear filter applied to the trial emissivity. In this case, the filter is a second order derivative operator. The chosen temperature is the one showing the smallest variance. The likeliest emissivity is computed from the measured radiance and the chosen temperature.

The two previous algorithms show some operation problems. For the ASTER algorithm, we observed a bias of at least 1 Kelvin that is superimposed on the resulting temperature. This bias was observed by Dash et al. [7]. The bias also affects the emissivity. The algorithm also generates numerical overflow error when the emissivity is low. The problem arises from the second block of the algorithm where, using the emissivity shape characteristics, the algorithm sets the minimum of emissivity. If the emissivity is too flat, the algorithm sets the minimum at a too high position and the temperature satisfying the Planck law become complex valued. It has not originally

been designed for processing low emissivities. It has instead the objective of providing results in the case of natural materials. For large pixels such as ASTER footprint, it is not likely to have low emissivity, because this type of material (e.g. metallic surface) is not often met in natural scene. In the case of the ISSTES, the appeal of the assumption is diminished when there is even a small error in the atmospheric irradiance estimation or if the sensor is a bit noisy. In these cases, the smoothing filter is not well behaved and reduces the algorithm convergence capability.

Iterative spectral smoothness assumptions are however very interesting and we decided to use them in another way. Instead of using a linear filter, that behaves like a second order derivative finite-difference filter, we prefer to filter the emissivity differently. We then compute a new radiance to obtain the total square error associated with the filtered emissivity. The technique behaves better near the likeliest temperature than the original ISSTES algorithm. One of the most interesting feature of this technique, is its behaviour with temperature. It enables the use of a fast procedure to identify the best temperature even with very noisy signals or large atmospheric errors.

A good algorithm can be stated as having three main characteristics. The first is the resistance to noise. The second is the ability to provide a realistic result even with high error on atmospheric characterization. The third is a behaviour enabling fast convergence toward likeliest temperature. Another interesting feature is the ability to work with a variable spectral resolution. The AIR-PIRATE sensor will need such a capability. Its signal-to-noise ratio will decrease with an improvement in spectral resolution. Resistance to noise feature of the TES technique is mandatory in this context. The resistance to atmospheric characterization error is needed because atmospheric models are still in a development phase and even if they were completed there will remain an error in the acquisition of the atmospheric profiles or on their determination using the image itself.

The algorithm described in the following pages uses iteration on temperature scheme similar to ISSTES. It is very resistant to noise. It is also resistant to atmospheric characterization errors in the sense that there will still be realistic results when the atmospheric characterization is completely wrong. It shows a capability to adapt to high or low spectral resolution. Finally, its behaviour is stable enough that it could be used with a fast temperature determination technique.

This memorandum is arranged as follows. It first describes the design of the algorithm. Afterwards, it shows results confirming its robustness to noise and atmospheric characterization errors. It then presents some results and a critic where it does not behave so well. Finally, it provides a conclusion.

2. Basis for algorithm design

This chapter describes the underlying assumptions and phenomenology under which a TES algorithm must operate. It also describes the iterative process of temperature estimation. It finally includes a description of the structure of the new algorithm. The technical details of the implementation are not described in this chapter but in chapter 3.

2.1 Theoretical foundations

2.1.1 Radiative transfer

We first assume that the atmospheric correction of the hyperspectral image was correctly applied. It means that there were no errors in the estimation of the transmittance and path radiance during the atmospheric compensation of the image, from which we obtain the ground leaving radiance defined as:

$$R = \varepsilon B + (1-\varepsilon)\frac{E_s}{\pi} \quad (1)$$

where R is the radiance just above ground level, B is the blackbody radiation function, ε the emissivity of the sample and E_s is the sky downwelling irradiance. The π factor is there because we assume the sample is a lambertian surface. The sky downwelling irradiance is the combination of the sun irradiance and the thermal irradiance for the sky itself. Even if the sun possesses a large radiance in the thermal infrared, its irradiance could easily be ignored when compared with the total atmospheric irradiance. Using equation (1), the channels from which a sensor makes its measurements becomes:

$$R_n = \int_{\nu_{on}}^{\nu_{1n}} \left(\varepsilon(\nu)B(\nu) + (1-\varepsilon(\nu))\frac{E_s(\nu)}{\pi} \right) w_n(\nu)\, d\nu \quad (2)$$

where ν denotes the wavenumber. $w_n(\nu)$ is a weighting function corresponding to n^{th} channel response. If we consider the different components of this equation to be constant on the interval over which the channel is defined, it could be simplified to yield:

$$R_n = \varepsilon_n B_b + (1-\varepsilon_n)\frac{E_{sn}}{\pi} \quad (3)$$

In the remainder of the document the π factor is incorporated inside the downwelling irradiance term. In this context the irradiance will be considered to be radiance. We can do that since the surface is considered to be lambertian. Equation (3) is a simplification of the complete radiance equation and could generate errors in the

estimation of emissivity. However, since equation (2) cannot be easily inverted with respect to emissivity, we use instead equation (3). Once the temperature is known, the emissivity could be computed using the following expression:

$$\varepsilon_n = \frac{R_n - L_{sn}}{B_n - L_{sn}} \quad (4).$$

2.1.2 Iteration on temperature

One of the common bases between our technique and ISSTES is the iteration on temperature. To do this, we must use a criterion to detect the best temperature. Usually a criterion could not be defined alone, some features of the signal must be removed or enhanced to increase the detectability of the correct emissivity. Borel uses a filter to remove the slow variation component of the emissivity. His criterion to choose the adequate temperature is the variance minimum of the filter output. Our criterion is different. We use the minimum of the total quadratic error between the measured radiance and a trial radiance computed with the filtered emissivity. The applied filter is built using a polynomial smoothing process.

If the function determining the criterion possesses a convenient behaviour, in the sense that it only shows one absolute minimum and no local minima, a fast minimum finding method could be used. The algorithm will be slow if instead it possesses multiple local minima, because we need to find the absolute minimum. Therefore, the iteration step can be adapted to the expected behaviour. Simulations have shown that our technique enables larger temperature steps when compared with ISSTES.

2.2 Description of ISSTES algorithm

ISSTES computes its smoothness criterion using the variance of the result of the application of a linear filter on the emissivity computed in (4). The filter is defined as:

$$s_n = \varepsilon_n - \frac{\varepsilon_{n-1} + \varepsilon_n + \varepsilon_{n+1}}{3} \quad (5).$$

ISSTES smoothness criterion is computed as the variance of the s_n values from n equal 2 to N-1, where N is the number of channels used in the TES operation. This operation implies the loss of two values from the extremity of the emissivity vector. Expression (5) could be rearranged like this:

$$s_n = \frac{-\varepsilon_{n-1} + 2\varepsilon_n - \varepsilon_{n+1}}{3} \quad (6)$$

By comparison a second order finite difference derivative is given by:

$$y''_n = \frac{x_{n-1} - 2x_n + x_{n+1}}{\Delta^2} \quad (7)$$

Where Δ is the width of the sampling interval. The behaviour of the ISSTES filter is the same as the second order signal derivative. It is very sensitive to noise. Looking at equation 7, we see that if the sampling interval is 1, then the variance of a filtered white noise sequence will be six times higher than the variance of the original sequence. This constitutes the lower limit of the variance. Generally, we obtain for the variance a figure that looks like Figure 1 in which there is a steep slope on the left side of the minimum and a gentle one on the right side. The minimum is not very well defined and the effect of noise could even decrease the slope on the right side as we can see in Figure 2. In Figure 2 we see outcomes of simulations where the same signal is corrupted with additive white noise. The noise amplitude is 1/250 of the blackbody emission computed at 293K. We can see that, in some cases, it may be impossible to find a minimum for the variance. That is due to the effect of the filter on the emissivity. The results shown in Figure 2 motivate our design of a new algorithm.

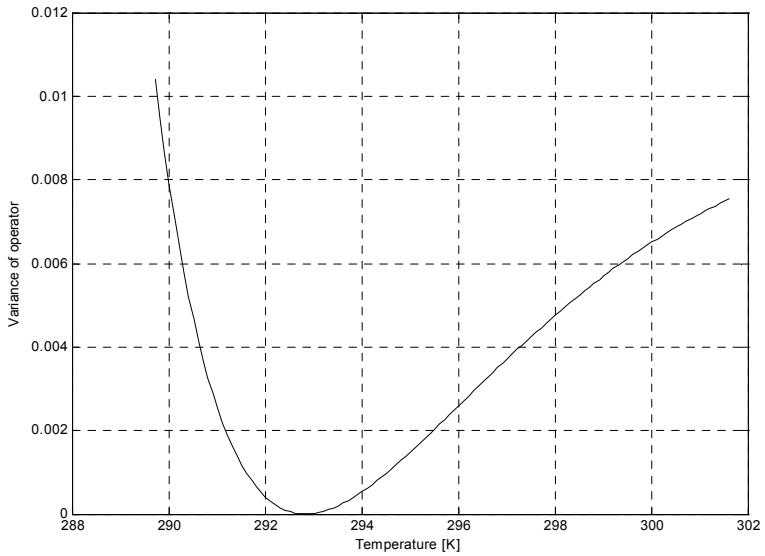

Figure 1: Variance as a function of temperature for a clean signal without noise

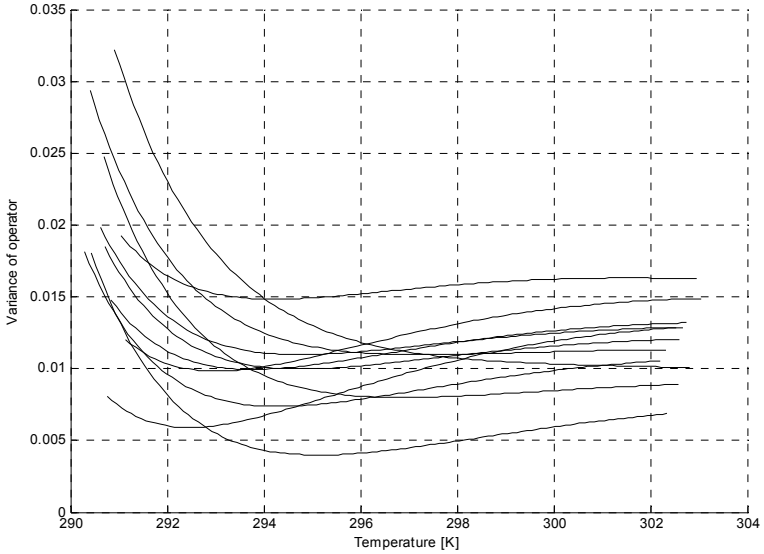

Figure 2: Variance as a function of temperature for the same signal as Figure 1, for 9 cases of noisy degradation. The noise level of the sensor is 1/250 that of a 293K blackbody. Only the random sequences change.

2.3 New technique description

We developed a different way to use the smoothness assumptions. The response of the filtering process must be considered carefully. A second order derivative filter increases the noise level and lower the signal-to-noise ratio when compared with a band-pass or even an all-pass filter. The filter used in ISSTES is a second order derivative filter. The frequency response of this filter decreases the signal to noise ratio by a very important factor. The emissivity cannot be considered to be stationary in the wavenumber domain. A linear filter, for which, every emissivity value has the same importance is therefore inadequate. We want to use every spectral band, because in low spectral resolution every band counts. ISSTES systematically loses the end bands for each measurement, which prevents its application to small band count hyperspectral data. With these considerations in mind, we decided to use a smoothing technique involving a polynomial fit of the emissivity computed using equation (4). The fitted emissivity is then used to compute back the radiance values. The likeliest temperature is the one that minimizes the total quadratic difference between the measured radiance and the computed radiance. The computed radiance is obtained using equation (3) where the emissivity is replaced by the smoothed emissivity. Figure 3 shows the flow of the algorithm for a given pixel.

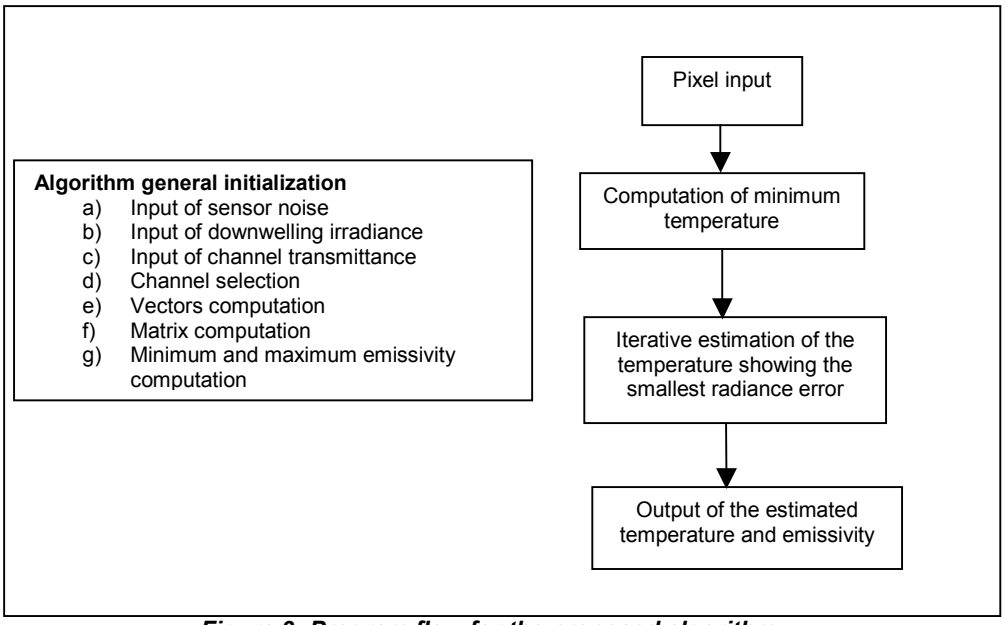

Figure 3: Program flow for the proposed algorithm

The following list enumerates the function to be implemented inside the algorithm. Some are done only at the initialisation and others are done for each pixel.

1. Initialization of the algorithm
2. Initialization of pixel processing.
3. Computation of the emissivity
4. Smoothing of the emissivity
5. Computation of new radiance
6. Computation of the error
7. Choice of a new trial temperature

To summarize the algorithm description, one must remember that the key features of the algorithm are the criterion and the filter used to smooth the emissivities. The criterion is the minimum total squared error. The last list describes all the elements that must be included in the implementation of the algorithm. All the implementation details are described in the following section.

3. Algorithm implementation

This section provides the description of the implementation details of the algorithm. It includes the design of all the building blocks and the motivation for the choices we did whenever it is necessary.

3.1 Initialization of the algorithm

The initialization of the algorithm is done using primarily the sensor characteristics and the atmospheric radiative transfer parameters such as the sky downwelling irradiance and the transmittance. The sensor characteristics are the spectral response of the channels and the noise added by the sensor. The radiative parameters can be obtained from various sources. Actually, we use radiosoundings acquired in the period near the acquisition of image data to compute the radiance and transmittance. Atmospheric parameters could however be acquired differently. In order, the following tasks need to be done: input the transmittance, input the downwelling irradiance and input the sensor noise. Once these steps are done, the channel selection is done using the sensor noise and the atmospheric transmittance. The sensor noise appears to be amplified when the atmospheric correction, to obtain the ground-emitted radiance, is done on the measurement. Therefore the noise levels are not the same; the ground-emitted radiance noise also depends on the transmittance of the channel. These variables are related by:

$$R_m = G_l \tau + R_p + N \quad (8)$$

where R_m is the measured radiance, G_l is the ground leaving radiance, τ is the transmittance R_p is the path radiance and N is the sensor noise. Inverting this equation to obtain the ground leaving radiance corrupted by noise, we obtain:

$$G_l = \frac{R_m - R_p}{\tau} - \frac{N}{\tau} \quad (9)$$

The noise term for the ground leaving radiance is the sensor noise divided by the transmittance. It means that, in circumstances of low transmittance, the signal to noise ratio of the ground leaving radiance will be too low. When this happens it may be better to discard the channel rather than using it and corrupting the whole process. The choice should be done with the signal to noise ratio in mind. For example, in our simulation we considered that the noise level of the sensor was 1/250 the signal level of a blackbody at 293K. It roughly means that with a transmittance of 0.4, the SNR will be of 100 for the ground leaving radiance. All the data with transmittance below or equal to 0.4 are discarded because of this too low signal-to-noise ratio. It is actually an ad hoc threshold. More work is needed to select a better threshold. Another possibility is to insert a weighting function to the error computation associated with the noise. The weighting function would depend on the noise level and transmittance of the channel. We decided to discard the too noisy channels because of their impact

on the polynomial coefficients estimation. The noisy channels possess a bad influence and should be ignored unless a good weighting scheme is designed to diminish the problem.

3.1.1 Vector and matrix computation

The polynomial-smoothing filter requires some computation during the initialization phase of the algorithm. Fundamentally the filtering process consists in 1) computing a set of coefficients for the polynomial that represents the best fit for the emissivity and 2) computing back that polynomial at each original wavenumber values. This process is described in many textbook, however, we reproduce it here, in order to highlight the important features of the computation.

The process starts with a set of measurement $\{x_n, y_n\}$ for which a function that models the y_n with respect to the x_n (the channel centers vector) is required.

The polynomial estimate of y_n is defined by:

$$\tilde{y}_n = \sum_{i=0}^{I} a_i x_n^i \quad (10)$$

The problem is to determine, according to the data, the coefficients a_i that give the best fit for the polynomial. We use for this purpose the least squares criterion. The total square error is defined as:

$$E^2 = \sum_n \left| y_n - \tilde{y}_n \right|^2 = \sum_n y_n^2 - 2\sum_n y_n \sum_{i=0}^{I} a_i x_n^i + \left[\sum_{i=0}^{I} a_i x_n^i \right]^2 \quad (11)$$

This function describes a quadratic surface in I+1 dimensions where I is the polynomial degree. It must be derived with respect to the polynomial coefficients a_i. Thus we obtain a linear system described by:

$$\boldsymbol{v} = \boldsymbol{M}\boldsymbol{b} \quad (12)$$

where $v_j = \sum_n y_n x_n^j$ and $M_{ji} = \sum_n x_n^{j+i}$ and finally $b_i = a_i$. To obtain the coefficients, one only has to compute the inverse matrix of M: $Q=M^{-1}$ and compute the vector v_j at each iteration.

The following steps describe the matrix and vector computation part of the initialization.

1) Compute the power from 0 to I of the channel center vector (x_n) and keep those values for use in the algorithm operation, they will form the v^{th} vector set $\{x_n^{\,i}\}$;

2) Compute the sum of the power of the vector x_n from the power 0 to the double of the polynomial degree. They will form the matrix ***M***.

3) Invert the matrix ***M*** and keep the result for algorithm operation.

The matrix M possesses the rank I+1. Since the elements of that matrix are the sum vector values at the power computed from their matrix position index, an increase in the size of the matrix reduces our capability to invert it. The matrix becomes badly conditioned with an increase in its size. This fact imposes a maximum value to the polynomial degree, which must generally be kept below 6 to avoid bad conditioning.

The final step, in the initialization procedure of the algorithm, is the computation of the minimum and maximum of the emissivity according to the sensor noise characteristics. We need in this step, guidance for the tolerable emissivity extreme values. For this purpose, we need to use an arbitrary temperature that could not be stated easily. The temperature can be defined using various ad hoc criterions in accordance with certain assumptions. One interesting criterion is the minimum equivalent temperature observed in the image because; the minimum temperature implies the minimum signal-to-noise ratio. The equation describing the transfer of the sensor noise to the emissivity is:

$$\varepsilon = \frac{R - L_s}{B - L_s} + \frac{N}{\tau(B - L_s)} \quad (13)$$

The second term in the right member contains the effect of noise. The only unknown in this equation is B the blackbody radiation because the temperature of the material under observation is unknown. In only very rare occasions the temperature of a pixel will be lower than the sky downwelling irradiance equivalent temperature. The lower B, the higher will be the effect of noise on the emissivity. The emissivity, of the material represented by the first term of the right member, could be 1, even if that situation is very rare. The emissivity defined in eq. (13) can therefore be superior to one, because of the sensor noise. The maximum emissivity could therefore be set according to the following equation:

$$\varepsilon_{\max} = 1 + F\left|\frac{\sigma_n}{\tau(B - L_s)}\right| \quad (14)$$

The standard deviation of the noise of the emissivity is computed using (13) as:

$$\sigma_\varepsilon = \frac{\sigma_n}{\left|\tau(B - L_s)\right|} \quad (15)$$

Where B is set at a value corresponding to the lowest possible temperature and F is a tolerance factor chosen by the user. Its value depends largely on the knowledge of the user about the sensor noise characteristics.

The minimum emissivity could also be set similarly. However this time, the minimum emissivity could be inferior to zero because of the effect of noise. The equation for the minimum emissivity is then:

$$\varepsilon_{\min} = -F\left|\frac{\sigma_n}{\tau(B - L_s)}\right| \qquad (16)$$

The importance of the maximum emissivity lays in the selection of the minimum temperature at which the algorithm will start at the beginning of each pixel processing. Its value needs to be computed for each sensor channels.

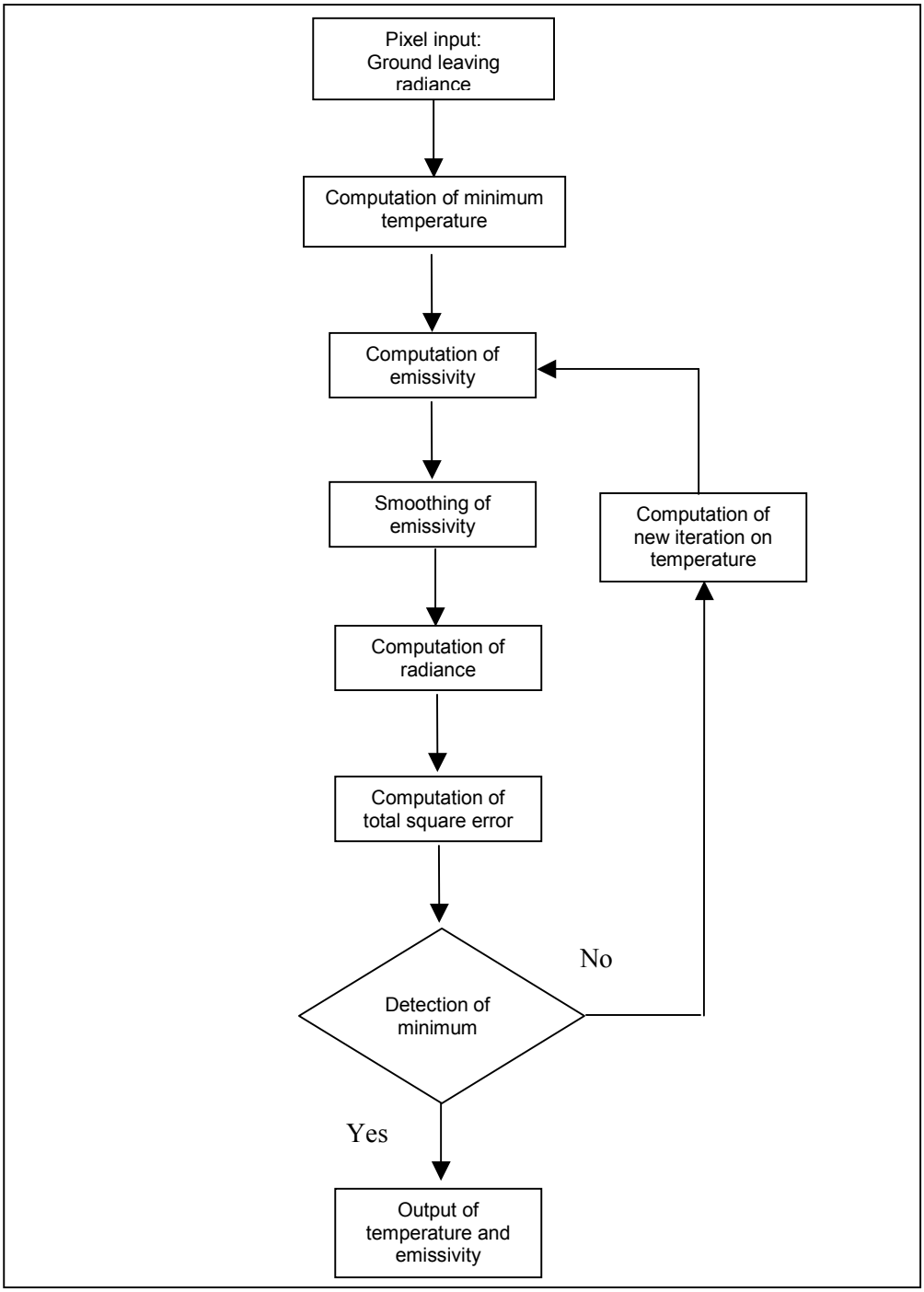

Figure 4: Detailed algorithm of the pixel processing

3.2 Pixel processing

In the previous section, the initialization phase of the algorithm is described. The object of the present section is to describe the operation of the algorithm (pixel processing). The pixel processing objectives are to obtain a temperature value and an emissivity set. One temperature value is needed for a given pixel while a set of emissivity values, one for each channels of the sensor, is needed. To obtain the temperature and the emissivities, a process has been designed. This process starts when a radiance measurement is introduced into the algorithm. The lower limit for the temperature is the first computation. It is done with eq. 17.

$$T_{\min} = \min\left[B^{-1}\left(\frac{R_n - (1-\varepsilon_{\max,n})L_{sn}}{\varepsilon_{\max,n}} \right) \right] \quad (17)$$

Where $\varepsilon_{max,n}$ is the maximum value the emissivity could take at the n^{th} wavenumber bin. It is obtained using equation (14). The minimum temperature computation constitutes the initialization of the pixel processing described in Fig. 4. In the following pixel processing, temperatures are selected using a minimum search technique based on the total quadratic error.

A loop follows the initialization. The first task, performed in this loop, is the computation of an emissivity value. It is done using equation (4). Afterwards, the emissivity is smoothed using the following procedure that begins with eq. 18.

$$s_i = \sum_{n=0}^{N} \varepsilon_n x_n^i \quad (18)$$

The *s* vector is a column vector of intermediate values used in the polynomial fit. Its component number is the degree of the polynomial plus 1. The x_n^i is the n^{th} wavenumber elevated to the power *i*. The polynomial coefficients, then, are computed using the matrix *Q* and the *s* vector

$$\boldsymbol{a}_j = \sum_{i=0}^{I} \boldsymbol{Q}_{ji} \boldsymbol{s}_i \quad (19),$$

and finally the smoothed emissivity is computed using the polynomial coefficients.

$$\varepsilon_n' = \sum_{i=0}^{I} a_i x_n^i \quad (20).$$

This procedure is equivalent to the computation of a large square matrix with the size of the emissivity vector, which is computed as follows:

Let $\boldsymbol{X}$ be the rectangular matrix for which each line is the power of the vector x_n. The number of lines is equal to the polynomial degree increased by one. The smoothing matrix is obtained using the steps given above. It has the form:

$$\varepsilon_{\boldsymbol{n}}^{'} = \boldsymbol{G}\varepsilon \quad \text{Where } \boldsymbol{G} = \boldsymbol{X}^{\boldsymbol{T}}\boldsymbol{Q}\boldsymbol{X} \quad (21)$$

The $\boldsymbol{G}$ matrix is a square matrix that has the same size as the emissivity vector dimension. However, the $\boldsymbol{G}$ matrix rank is determined by the rank of the $\boldsymbol{Q}$ matrix and is the same as the degree of the polynomial plus one. $\boldsymbol{X}^{\boldsymbol{T}}$ is the transpose of the $\boldsymbol{X}$ matrix. There could be an operational gain in using directly the $\boldsymbol{G}$ matrix as a linear filter, but it is interesting only for large polynomial values and small channel numbers. What makes the interest of the smoothing matrix is that it enables the study of the whole process in a simpler way, noting that the complete smoothing process is in fact the application of a linear filter to the trial emissivity. This study will lead to more interesting filters, optimized for atmospheric effect reduction or noise mitigation.

The following step is the computation of radiance using the smoothed emissivity. This is done using eq. 3 and the smoothed emissivity. The new radiance could be written as:

$$R'_n = \varepsilon'_n B_n(T) + (1 - \varepsilon'_n) L_{sn} \quad (22)$$

The total quadratic error is computed as a function of temperature. It is given by:

$$E^2 = \sum_n \left[R_n - R_n'\right]^2 \quad (23)$$

Equation (23) is the sum of quadratic differences. The fact that the modeled emissivity could have an offset compared with the true emissivity is handled by the return to the radiance domain using the trial temperature. The total quadratic error could also be replaced by the total absolute value of the differences. In this case, there are only marginal differences between the two schemes. Instead of an error on radiance, the difference between the trial and filtered emissivity could be used as the temperature selection criterion. The reason why the error on radiance his used lies in the fact that noisy bands see their influence reduced, when compared with the difference in emissivities. The differences between these computations are illustrated below. Mathematically the emissivity change could be stated as:

$$E_\varepsilon^2 = \sum_n \left(\varepsilon_n - \varepsilon'_n\right)^2 \quad (24)$$

where

$$\varepsilon' = G\varepsilon \quad (25)$$

G is the operator representing the filtering process. The error on the radiance could be represented as follows:

$$E_R^2 = \sum_n \left(R_n - \varepsilon_n'(B_n - L_{sn}) + L_{sn}\right)^2 \quad (26)$$

The radiance at channel n could be replaced with the parameters used to compute it. E_R leading to the following expression:

$$E_R^2 = \sum_n \left[(B_n - L_{sn})^2 (\varepsilon_n - \varepsilon'_n)^2\right] \quad (27)$$

Which is almost the same as equation (24) with the exception of the weighting function composed of the difference between the blackbody radiation and the downwelling irradiance converted into radiance. This weighting function depends on a slowly varying function, the blackbody relation, and the sky irradiance, which varies faster. Most of the time the temperature of the ground will be higher than the apparent temperature of the sky. However, at low atmospheric transmittance the atmospheric irradiance will be at its highest point, so the weighting function will be small. The noise level possesses its largest value at low transmittance. Equation 27 provides a natural consideration for noise. This way, some very noisy channels are usable and their effects mitigated in the error computation when compared with the less noisy channels.

3.2.1 Minimum search and selection of new temperatures

One of the strength of this method is the fact that the error computed with equation (21) is generally well behaved. It is smooth with temperature. Its shape is very similar to a parabola in the temperature region of interest. This is true even with very noisy signals. This behaviour enables the use of fast minimization algorithm of the error. The fast technique could be used with a very noisy signal and large errors in atmosphere downwelling irradiance estimation. In the initialization procedure done for each new pixel, we have computed the minimum possible temperature. This value is the starting point for the minimum search algorithm. In the following the search technique is described.

Start at the minimum temperature value;

Set the temperature step to 1K;

Compute the total quadratic error;

Repeat the sequence of increasing the temperature by one step and compute the total quadratic error until the error begins to increase;

Reduce the temperature step by a factor of 10;

Reduce the temperature by one step and keep reducing the temperature until the error begins to increase;

If the error increasing behaviour began at the first iteration increase the temperature by one step until the error starts to decrease;

Reduce the temperature by one step. This is the minimum temperature.

The application of this procedure will lead to evaluations of the error approximately 20 times per pixel. The number of times the error has to be estimated can be reduced with the use of a better minimum search technique.

3.3 Polynomial degree

A polynomial of a too low degree will not enable the modeling of some emissivities, while a too high degree introduces a too good modeling of computed emissivities and the remaining atmospheric features contained in the computations. There is another reason for keeping the polynomial degree low. In the initialization a matrix needs to be inverted. It is notorious that the matrices used in polynomial fitting are frequently not well conditioned. This problem increases with the high polynomial degree. Computation tricks may be used to reduce this problem.

3.4 Conclusion

The implementation details of the algorithm have been described in this chapter. The technique initialization procedure, the initialization of the pixel processing, the process itself, the decision rule for the choice of the pixel temperature and the use of the quadratic error have been described. To remove the atmospheric features from the emissivity, a polynomial fitting technique is used. The hypotheses behind this choice are that at the right temperature the trial emissivity will contain a very small amount of atmospheric feature and that the materials emissivities are smooth when compared with the atmospheric features. The material emissivity will not be modified by the use of a sufficiently low degree polynomial. It implies that the differences in the radiance domain between the measurement and the smoothed emissivity computed radiance are minimum at the adequate temperature. The emissivity filter possesses a tremendous importance because it is the key element for determining stability, accuracy and noise sensitivity of the algorithm.

A stable error function enables the use of a fast minimum search technique. This search technique, while secondary in importance to the precision has been described in this chapter. It also includes the decision rule for selecting the correct temperature. The gradient technique is not used because an analytical expression for the error does not exist. Instead, an iterative method is used. It is based solely on the computation of the quadratic error.

4. Robustness of the algorithm to noise and atmospheric modeling errors

An interesting characteristic of a TES algorithm is ability to work in very adverse conditions: it must provide results as accurate as possible for inputs that are not accurate. Three major impairments could affect the signal. The first is the noise generated by the sensor. The second is the inaccuracy of the downwelling irradiance at the input of the algorithm. Finally, the third impairment is the incorrect atmospheric correction (wrong estimation of path radiance and transmittance) of the pixel. Inaccuracies in estimation of atmospheric optical parameters occur generally because the atmosphere is not well modeled or the radiative transfer model is wrong. Since the error in atmospheric correction increases with altitude, a satellite born sensor will suffer more than a low altitude airborne sensor. The error in estimation of downwelling irradiance, however, does not depend on altitude. It has a higher effect on low emissivity targets. If the downwelling irradiance estimation is erroneous, it is very unlikely that the estimation of other atmospheric optical parameters would be good. The largest difficulty in estimating the robustness of a TES algorithm to inaccuracies in atmospheric modeling arises from the present incapacity to model them. The errors are largely dependent on the used atmospheric correction algorithm and they have to be characterized on that basis. Attention has been directed at robustness to errors in downwelling irradiance estimation and a simulation approach has been used.

4.1 Simulation description

The TES technique seems quite robust in a number of operating conditions. A stressing atmospheric model, the MODTRAN tropical model, is used. It is stressing on the algorithm because it lowers the contrast between the blackbody radiation emitted at the ground temperature and the atmospheric downwelling irradiance. The sensor is positioned at a 10 km altitude for transmittance computation. The simulated sensor is a FTIR having bandwidths of $4cm^{-1}$ and channels going from 800 to 1250 cm^{-1}. The channels showing a transmittance lower than 0.4 are eliminated in the channel selection step as this has been discussed in the previous chapter. The experiment characteristics are the following:

- About the sensor:
    - FTIR sensor with 4 cm^{-1} channel bandwidth
    - Noise level corresponding to 1/250 of the 293K blackbody
    - Position of 10 km above ground
- About the targets
    - Temperature of 293K

- Emissivity extracted from the ASTER Library

- About the atmosphere
  - Simulation atmosphere is MODTRAN standard tropical
  - Adverse atmospheric conditions
    - MODTRAN tropical +2 degree temperature offset
    - MODTRAN tropical –2 degree temperature offset
    - MODTRAN mid-latitude summer

To estimate the temperature selection accuracy, three simulations have been selected. The first one had the objective of to verify the effect of noise on the temperature estimation. The second one aimed at estimating the algorithm robustness to atmospheric modeling errors. The objective is the verification of the stability of the algorithm when the error of atmospheric downwelling irradiance is high. The measured radiance is simulated using the MODTRAN tropical atmosphere model, while the downwelling irradiance is computed using the MODTRAN mid-latitude summer model. The last simulation is the most streesful case for the algorithm; random noise is added to the second simulation measured radiance. To illustrate the results, the computation done with a colemanite emissivity "colemac.txt" extracted from the ASTER spectral library is used.

4.2 Algorithm resistance to noise

The first studied simulation is the noise simulation. It is performed with the use of all the samples contained in the ASTER spectral library. In all cases the algorithm converged to a valid value, which means a clear minimum error.

Figure 5 shows the error curve as a function of temperature for an ideal case, without noise or atmospheric error. The inability of the smoothing filter to model perfectly the emissivity of the colemanite explains the remaining error at the minimum position. It also explains the temperature estimation error. The temperature should be 293K. Remember that the objective of the filter is not to model accurately the emissivity; it is the removal of the atmospheric residues in the computed emissivity. This introduces errors in the results whenever there is a sharp variation in the emissivity.

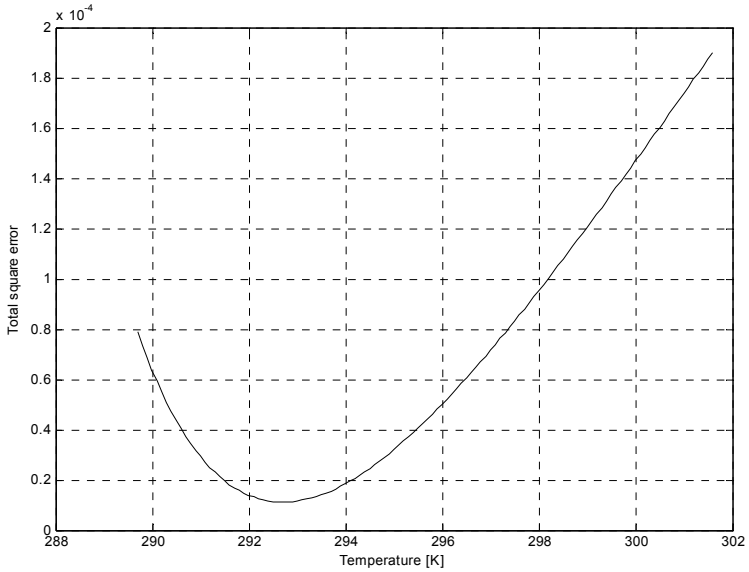

Figure 5: The error as a function of temperature for the sample of colemanite

Noise introduces errors in the signal. These could be interpreted as atmospheric features in the computed emissivity by the algorithm. The random noise generated by the sensor possesses a different behaviour compared to the atmospheric features. Its mean is null and its standard deviation depends on the sensor noise and on the channel transmittance. Figure 6 shows for the colemanite sample some of the Monte-Carlo results in the experiment made with the use of the good correction atmosphere and measured radiance corrupted by noise.

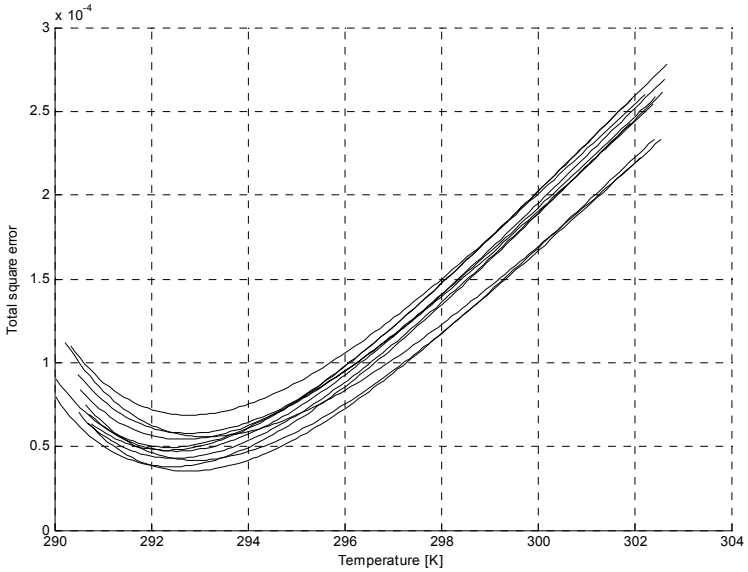

Figure 6: Error as a function of temperature for noisy data

The error floor, the temperature position and the sharpness of the error parabola, are all affected by noise, as it can be seen in Figure 6. The error floor is higher than what is observed in Figure 5. It does not influence much the algorithm's ability to find a minimum position. The temperature position is more influenced, since half a degree of precision must be tolerated with such a high noise level. The third effect, the broadening of the parabola could be interpreted as a decrease in stability of the algorithm because of the noise. If we compare with ISSTES in Figure 2, we see that this technique is more stable with the same input data.

4.3 Algorithm resistance to downwelling irradiance errors

A simulation performed with high atmospheric downwelling irradiance error is presented in Figure 7. To generate the measured radiance the MODTRAN standard tropical model and the MODTRAN standard mid-latitude summer atmosphere has respectively been used for the computation of the measured radiance and the correcting downwelling irradiance. Figure 8 shows, for the same set of atmospheric models, simulations performed with some noise added.

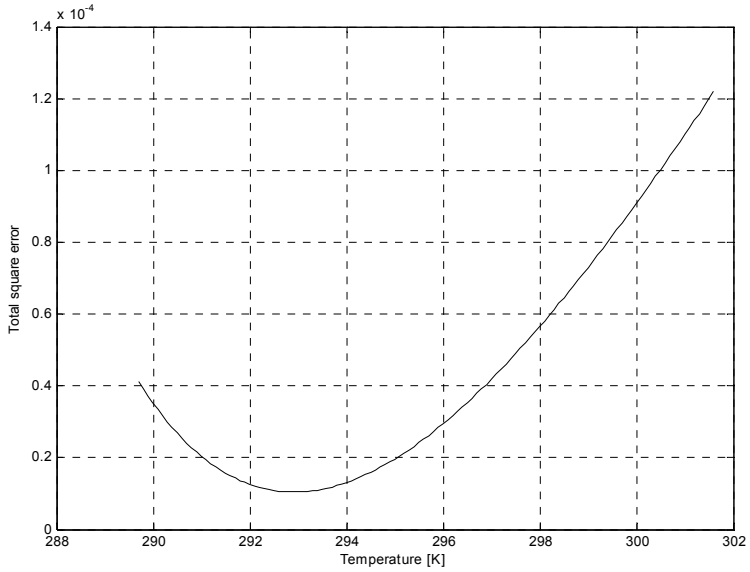

Figure 7: The error as a function of temperature for the sample of colemanite with the wrong atmosphere

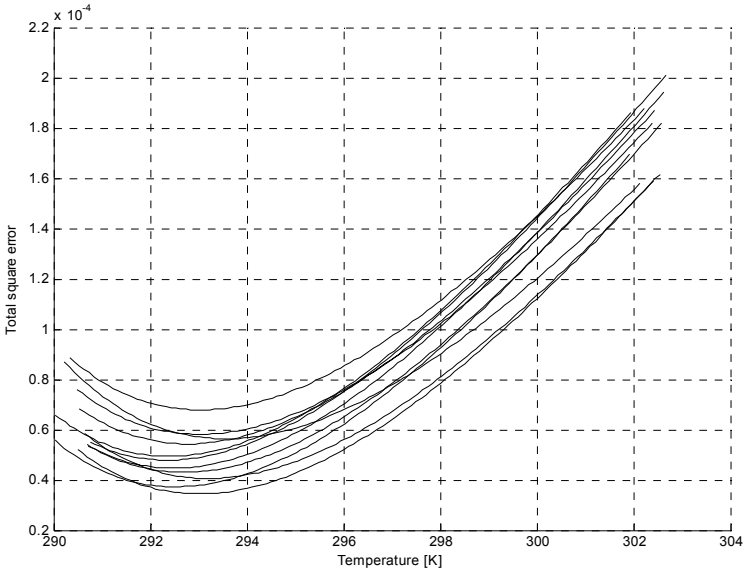

Figure 8: Some samples of the error as a function of temperature for noisy data and wrong atmosphere for the sample of colemanite.

These atmospheric conditions can be considered as extreme cases of error. Nonetheless, the algorithm still converges with stability toward credible values. The difference between Figures 7 and 5 is that the parabola is much wider in the first one. The position of the minimum for the choice of the temperature did not change much. It can be seen, from the comparison of Figure 8 and 6 that the width of the parabola increases further when noise is added. The width increase can be interpreted as a stability reduction of the algorithm.

4.4 Conclusion

It has been shown in this Chapter that the designed algorithm is quite resistant to sensor noise and to atmospheric downwelling estimation errors. The errors introduced by a wrong atmospheric correction are not considered in this chapter. The impacts of these last errors must be considered separately in conjunction with the algorithm that will be used for estimating the atmospheric correction parameters, the transmittance and the path radiance.

The objective of this section was to demonstrate the good behaviour of the algorithm in a wide range of conditions even in the case of large errors from both noise and atmospheric nature. The algorithm has demonstrated it has this capability. The demonstration is needed to provide some confidence in the possibility to use a fast minimum search technique to a multitude of cases. Confidence in the algorithm is well founded because the stability looks to be very high. However, one must not be too confident as some cases could exist that will prove to be wrong. To consider those probable cases, a feature for detecting an out of range temperature should be included inside the algorithm.

5. Critic of algorithm operation

In the previous chapter, the concern was to establish the stability of the algorithm when it is subject to strong errors. In this chapter the aim is to verify the susceptibility of the algorithm to impairments. The study is based on work already carried out on the Borel ISSTES algorithm by Ingram and Muse [6]. They provide an interesting way to analyze the results of a TES algorithm. In their work, three types of errors are identified depending on the algorithm operation or on its assumptions. The first kind of error is defined as the algorithmic error, i.e. the error generated solely by the use of the technique without any impairment and in the best possible conditions. This error is due mainly to the under-determinate nature of the algorithm. Measurement error such as the sensor noise constitutes the second kind of errors. Ingram and Muse considered this noise to be white and gaussian. The last type of error is the modeling errors, i.e. the errors caused by problems with atmospheric corrections techniques and the downwelling irradiance estimation errors or by any other pre-processing steps performed on the image. The atmospheric modeling error is due mainly to algorithmic error on estimation of atmospheric parameters such as the downwelling irradiance, the transmittance and the path radiance. They will be studied in conjunction with the atmospheric correction algorithms in future work. Another error is due to sensor calibration. It is supposed that the sensor is well calibrated spectrally and radiometrically because calibration errors are very difficult to characterize.

The error study is focused on the effects due to sensor noise and those of the variability in emissivity. To fulfill this task, a complete set of data has been generated by simulation. The emissivities contained in the ASTER spectral library are used; it represents a number of 1244 emissivity samples. The radiances are computed for a temperature of 293K at the surface and the use of MODTRAN standard tropical atmosphere for the other radiative transfer parameters. Some of the samples duplicate measurements of the same material in a different form, some are solid and others are powders. The atmosphere and ground temperatures were chosen in order to diminish the contrast between them. This setup stresses the algorithm because it decreases the signal-to-noise ratio for the ground leaving radiance. The dataset is then perturbed with white noise transferred from the sensor to the ground through the transmittance. A hundred sequences of noisy data were generated this way and recorded for future use. The algorithm is used with the complete dataset to obtain the results of algorithmic errors and the effects of sensor noise on the data.

5.1 Algorithmic error

The algorithmic error must be considered for both the temperature and emissivity even if these two errors are interdependent. A temperature error, for instance, will generate an offset on the emissivity. Ingram and Muse [6] evaluated the error in emissivity with root mean square (RMS). However, the use of an offset from the current computed emissivity to the sample emissivity is preferable since it is the kind of error that will generally be observed. The random noise introduces an error in the estimation of temperature. This error in temperature introduces an error in the emissivity

estimation. Since equation 15 suffices to describe the effect of noise on emissivity and that this error is linked to the error on temperature, the effort is concentrated on the evaluation of the error on temperature rather than on emissivity.

From the simulation results, using the ASTER spectral library, three groups of emissivity samples have been identified to cause high temperature errors. The first group generates errors that are more than 2K below the target temperature, the second generates errors 2K higher and finally the last group generates errors below 0.1K from both sides of the target temperature the remaining emissivity samples are generating errors below 2K but not outstandingly good estimation.

The first group is constituted of 9 samples. These are the files: olivin4t.txt; olivin6t.txt; olivin8t.txt; orthoc3s.txt; ps22ac.txt; s22am.txt; sanidi1s.txt; topaz1s.txt; vesuvi1s.txt. The emissivity of these samples all show very sharp transition from low to high emissivity or brutal changes of amplitudes. These could be difficult to model with our polynomial and so produce these types of errors. The largest error is given by ps22ac.txt and is of –3.08K. This sample is a kind of silicate material from India.

The second group generates errors that are larger than 2K. It is composed of 14 samples. These samples are: andrad1s.txt; bustam1s.txt; c02af.txt; clinoz1s.txt; hemimo1s.txt; hornbl3s.txt; natrol1s.txt; ns03bc.txt; ns03bm.txt; quartz1s.txt; richte1s.txt; tremol1s.txt; tremol2s.txt; zoisit1s.txt. Of these samples, zoisit1s.txt generates the largest error of more than 7K. It is followed in order by: natrol1s.txt; clinoz1s.txt and quartz1s.txt, which generates, respectively, errors of about:5.7K, 4.5K and 3.8K.

Zoisit1s is a silicate material from Tanzania. This sample represents the most difficult case for the algorithm to tackle. Figure 7 shows the emissivity of the sample. In the band of interest it has two deep valleys. These valleys are very deep and a polynomial of the fifth degree is not good for modeling it. Higher degree polynomials were tried to estimate the needed degree. A 15^{th} degree polynomial was needed to reduce the error made with the zoisit sample to an acceptable level. This polynomial also models too accurately the variations introduced by noise and atmospheric perturbations. It has to be discarded as a solution because of this behaviour. This kind of result, if occurring more frequently, will trigger the need for the design of a different algorithm more adapted to these situations. Adding together the samples generating high error levels, a number of 23 samples is obtained. When compared with the 1244 samples it means that less than 2% of the samples are causing errors exceeding a 2K limit.

The last group is composed of samples generating very small errors. That one is composed of 183 samples out of the 1244 processed samples. There is no need to enumerate them. However, their emissivity is generally very well behaved in the sense that they are very flat in most cases if they are low or they may vary but still stay at a high level above 80% emissivity. Of the 1244 samples processed 1221 samples stays below the +- 2K errors for the algorithmic error.

The error on emissivity depends on the error on temperature, especially if there is no error on the atmospheric downwelling irradiance. The fact that temperature is crucial

to the operation of the algorithm implies that if there is no error on the temperature there should also be no error on the emissivity other than what is introduced by noise. At 300K an error of 1 degree is likely to generate an error of approximately 2.5% on the emissivity at 1000 cm^{-1}. In Figure 9 the errors in emissivity are approximately of 16% for a temperature error of 2.5K. This error is spread evenly on the whole emissivity with differences generated by the shape of the blackbody function and atmospheric introduced feature. The emissivity of the Zoisit1s sample is given in Figure 9 and its error curve in Figure 10.

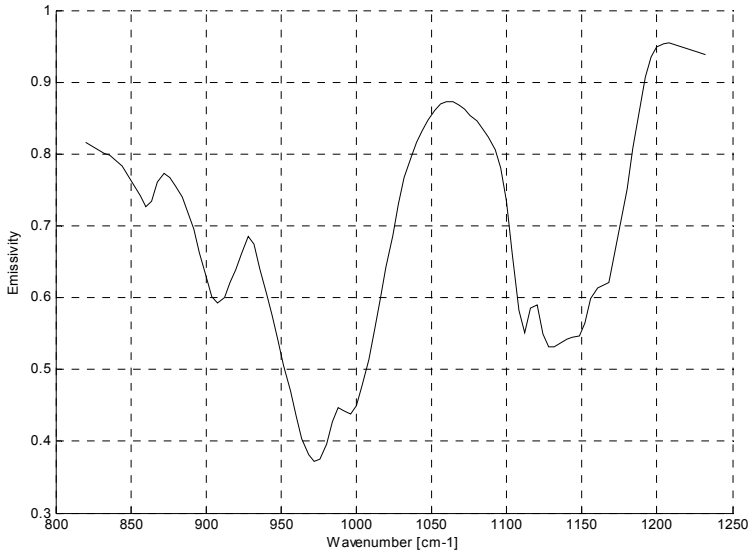

Figure 9: Emissivity of the Zoisit1s sample.

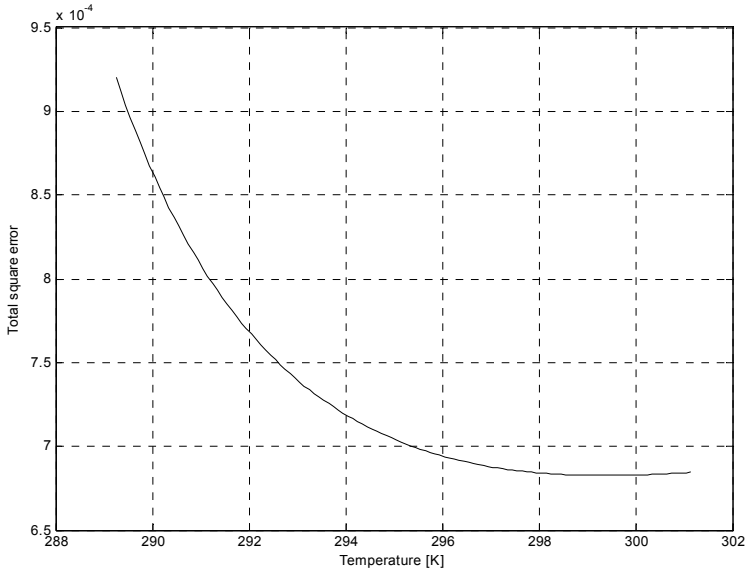

Figure 10: Error curve for the Zoisit1s sample

The error curve shows a minimum that is not well defined and largely above the simulation temperature. It is clear that noise will have a strong effect on that sample.

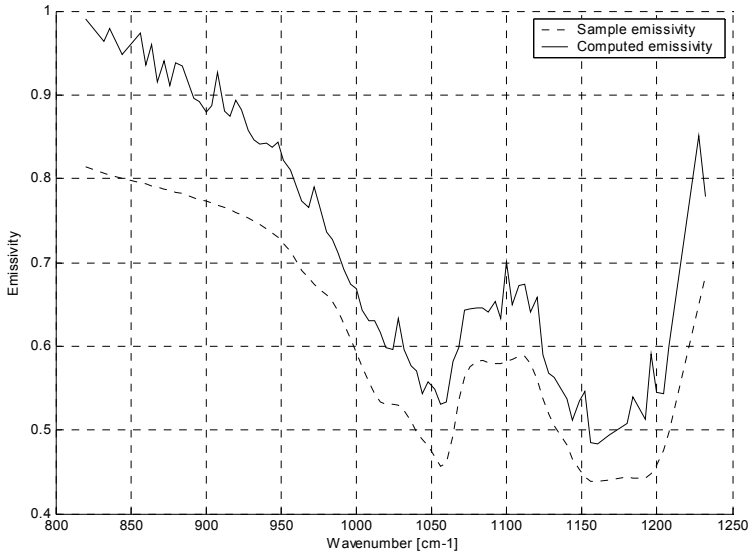

Figure 11: Error on emissivity for sample of orthoc3cs, estimated temperature 290.5K

Figures 9 and 11 shows samples of emissivity that generates high error levels. One common characteristic of these emissivities is that they have strong variations as a function of wavenumber. In the case of the sample shown at Figure 8, at least two local minima and two local maxima with a number of low importance local maxima and minima. For the ortho3c sample shown at Figure 11, there is 1 local maximum and 2 local minima with two ramps at the edges of the sample. We use in the algorithm a fifth degree polynomial for the representation of the emissivity. Such a function could possess only a total of four minima and maxima. It means that in such cases the fifth degree polynomial will not work and must be replaced by something else in the design of the filter. Nonetheless, the technique is promising in its actual form. It works well for low emissivity targets and for emissivities that do not change much, like vegetation.

5.2 Error due to measurements errors

In this section we consider only the random error made on the measurement. This error is considered as white gaussian noise generated by the sensor. Measurements are taken independently so there should be no correlation between measurement errors from one channel to the other. Ingram and Muse [6] used two procedures to estimate the retrieval error. They developed an analytical method based on the implicit function theorem for the estimation of the variance and bias of the error. They also used a Monte Carlo simulation to obtain the variance and bias due to noise. Even if the noise is additive and possess a zero average, a bias produced by non-linearity of the process could exists. This bias could be estimated with the use of a Monte-Carlo experiment.

Only the Monte-Carlo simulation was used to obtain the bias and the standard deviation of the error for the case of an already well-behaved sample of colemanite.

5.2.1 Monte Carlo experiment

The algorithmic error associated with the colemanite sample is -0.31 K. The simulation was launched using the already computed ground emitted radiance. The sensor noise was transferred to the ground with the use of the transmittance given in Figure 12. The determination of temperature is done 1000 times with a different noise vector possessing the same statistical properties. The mean of the error in temperature is computed to obtain the noise-generated bias and the temperature error standard deviation is computed for each noise level. Two figures, 13 and 14 have been generated. Figure 13 shows the bias due to noise and algorithmic error and Figure 14 is the standard deviation.

It can be seen from Figure 13 that the bias added by noise to the algorithmic error is very small except for high noise level and is smaller than the algorithmic error itself. For the standard deviation shown in figure 14 the noise has a more important effect. If an error of about 0.1 degree is tolerable due to the effect of noise then a signal-to-noise ratio of approximately 750 will be necessary. With an expected signal to noise ratio of 250 and the sensor at 10 km a standard deviation of 0.3 has to be accepted. If the transmittance is better or if the contrast between the atmospheric radiance and the ground radiance being larger, then a sensor could generate more noise and still produce the same result.

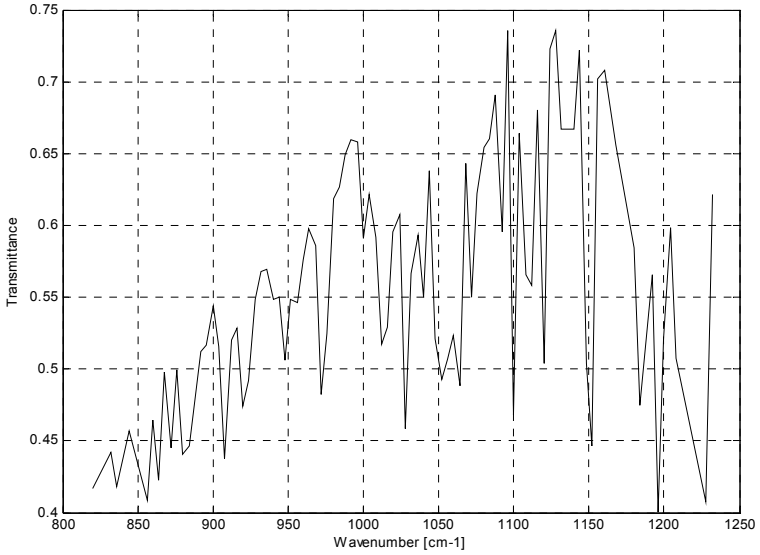

Figure 12: Transmittance for each channel

.

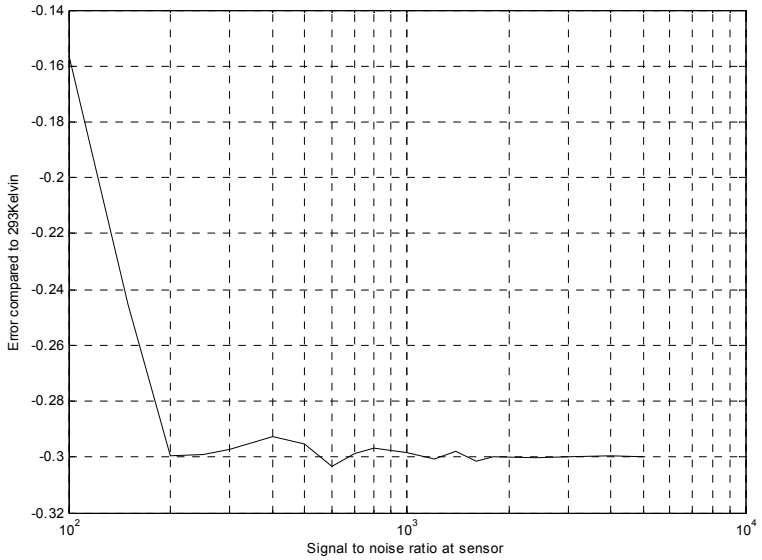

Figure13: Bias error for temperature as a function of signal to noise ratio

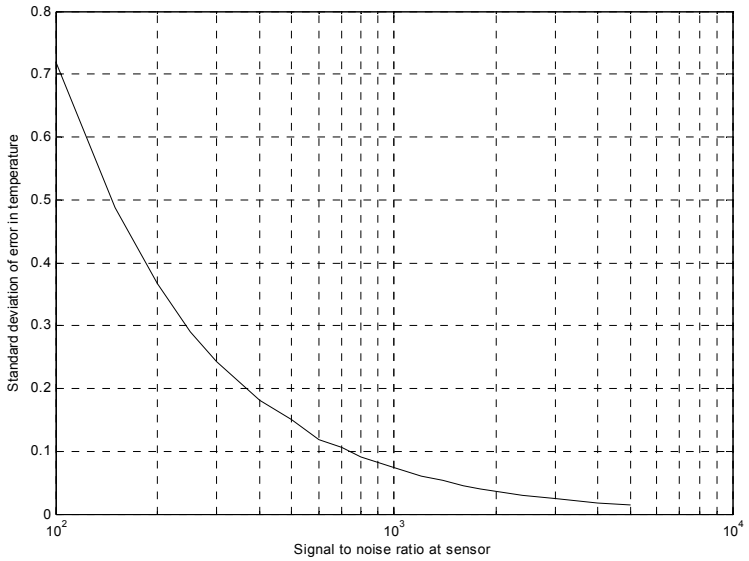

Figure 14: Temperature standard deviation as a function of signal to noise ratio

The consideration for the error on emissivity is still the same here as it was in the previous chapter. The variance at each channel value depends on the random noise statistics in the channel. If there is no bias introduced by the noise the offset error due to noise on emissivity will remain very low. There will only remain the offset error due to the algorithmic temperature error. The effect of noise on emissivity is to make it spiky. If an error due to temperature algorithmic error exists, then the remaining

atmospheric spikes will add to the noise spikes. To alleviate this problem one could use a noise reduction filter that will diminish the effects of the random noise and the impact of the variations in atmospheric downwelling irradiance.

5.3 Conclusion

In this chapter, simulations studying the behaviour of the algorithm relatively to algorithmic errors and noise have been performed. The algorithmic error is defined as the estimated temperature offset due to the operation of the algorithm on a given sample. It is due to the underdetermined nature of the TES problem. One goal in the design of a suitable algorithm is to reduce it as much as possible in most cases. The noise can introduce two forms of errors; a bias due to the nonlinear behaviour of the estimation technique and a random inaccuracy in the estimation of temperature. This last error is normal and constitutes a linear behaviour of the algorithm.

The simulations are using stressing conditions for contrast between the ground thermally emitted radiance and the incident irradiance from the sky. Nonetheless, the obtained estimation error on the temperature are in most cases below 2K. In some cases where the emissivity of the sample changes a lot the error is too large. The algorithm will have to be modified in order to provide better results in these cases.

Using a Monte Carlo simulation the effects of noise on the temperature estimation are assessed. It has been found that the noise-introduced bias on the temperature estimate is very small as shown in Figure 13. The linear error due to noise on the temperature estimate is more important as shown in Figure 14. To achieve a precision on temperature of 0.1K the required signal-to-noise ratio needs to be better than 750.

6. Conclusion

In this document a new technique for the separation of temperature and emissivity from the ground leaving radiance is described. To obtain the temperature, it looks iteratively for the temperature that minimizes an error criterion, which is the total squared error using the following procedure. The algorithm estimates the emissivity according to a trial temperature. It smoothes this emissivity using a polynomial linear filtering process similar to a matrix operator applied to a vector. The radiance is computed back with the smoothed emissivity. The error is the total of the square of the difference between the computed radiance and the measured radiance.

The algorithm is robust to noise and to strong error in atmospheric downwelling irradiance estimates. To characterize the operation of the algorithm with error in atmospheric parameter one will have to use particular atmospheric estimation algorithm in conjunction with the TES algorithm. The error function of temperature is well behaved in most situations. In simulations, even with a low signal to noise ratio the algorithm converge and there has been no situation where it had not converged in realistic noise and atmospheric errors situations.

The algorithm has similarities with the ISSTES algorithm from Borel [5]. The difference stands mainly in the way the sample temperatures are selected. In the Borel algorithm the trial emissivities are filtered using a numerical second order derivative. The temperature showing the minimum variance for this operator is selected as the adequate temperature. The Borel algorithm did not show the same convergence capabilities compared to our algorithm in noisy environments. A thorough study of the operation of both algorithms in the very same conditions is needed, however, to assess and compare their performance.

It is shown in the document that the filtering process used to smooth the emissivity has a tremendous importance in the behaviour of a technique and its susceptibility to noise. The filter used to do it must be designed in order to minimize the effects of the noise and the atmosphere without too much altering the underlying emissivity. Future work on this matter should be done with the goal of reducing as much as possible the algorithmic error on temperature and keeping a high resistance to noise. The importance of the filtering process constitutes the main theoretical observation made in the work leading to this document.

7. References

1. Guillaume Girard, "Conception du système d'imagerie hyperspectrale à transformée de Fourier MRSCAN", Rapport AEREX No: 2002-21098 version 1.0, contrat TPSGC W7701-2-1098

2. A.R. Gillespie, S. Rokugawa, S.J. Hook, T. Matsunaga and A.B. Kahle, "Temperature/Emissivity separation algorithm theoretical basis document, version 2.4", Report prepared for NASA under contract NAS5-31372, 22 March 1999.

3. A. Gillespie, S. Rokugawa, T. Matsunaga, J.S. Cothern, S. Hook, A.B. Kahle, "A temperature and emissivity separation algorithm for advanced spaceborne thermal emission and reflection radiometer (ASTER) Images", IEEE transactions on geoscience and remote sensing, vol 36, no 4, July 1998. pp. 1113-1126

4. A.R. Gillespie, S. Rokugawa, S.J. Hook, T. Matsunaga and A.B. Kahle, "Temperature/Emissivity separation algorithm theoretical basis document, version 2.3", Jet Propulsion laboratory, Pasadena 16 August 1996

5. Borel, C.C, "Surface emissivity and temperature retrieval for a hyperspectral sensor", Geoscience and Remote Sensing Symposium Proceedings, 1998. IGARSS '98. 1998 IEEE, International , Volume: 1 , 6-10 July 1998, pp. 546 -549 vol.1

6. Ingram, P.M., Muse, A.H, "Sensitivity of iterative spectrally smooth temperature/emissivity separation to algorithmic assumptions and measurement noise", Geoscience and Remote Sensing, IEEE Transactions on , Volume: 39 Issue: 10 , Oct. 2001, pp. 2158-2167

7. P. Dash, F.-M. Göttsche , F.-S. Olesen and H. Fischer, "Land surface and emissivity estimation from passive sensor data: theory and practice-current trends", International Journal of Remote Sensing, 2002 vol 23, no 13, pp. 2563-2594.

List of symbols/abbreviations/acronyms/initialisms

R: Ground leaving radiance
R_n: Ground leaving radiance for channel n
ε: Emissivity
B: Planck function
E_s: Sky downwelling irradiance
n: Wavenumber
n_{on}: Lower boundary for channel n
n_{1n}: Higher boundary for channel n
n: Index of channel
$w_n(\nu)$: Spectral response for channel n
E_{sn}: Total value of sky irradiance weighted by $w_n(\nu)$
L_{sn}: Radiance in channel n corresponding to sky irradiance reflected by a lambertian surface
s_n: Result for channel n of Borel's smoothing filter
y''_n: Second derivative filter result
Δ: Sampling interval
τ: Transmittance
R_p: Path radiance from the ground to the sensor
G_l: Ground leaving radiance
N: Sensor noise
y_n: Value of a function for channel n
$\tilde{\boldsymbol{y}}_{\boldsymbol{n}}$: Estimation of function in channel n
a_i: Polynomial coefficient
i: Polynomial power and index
E^2: Total square error
$\boldsymbol{M}$: Matrix
m_{ji}: Matrix element of matrix $\boldsymbol{M}$
ε_{max}: Maximum possible emissivity according to sensor noise
σ_e: Variance of emissivity
σ_n: Variance of noise in channel n
ε_{min}: Minimum of emissivity
T_{min}: Minimum temperature
B^{-1}: Inverse of Planck function
$\boldsymbol{Q}$: Inverse of matrix $\boldsymbol{M}$
ε_n': Smoothed emissivity for channel n
$\boldsymbol{X}$: Rectangular matrix, collection of vectors used in polynomial estimates
E_e^2: Total square difference of emissivities

Glossary

Radiance	The intensity of light per unit of solid angle and unit of frequency or wavelength or wavenumber
Irradiance	The total intensity of light incident on a given surface from all direction per unit of frequency or wavelength or wavenumber.
Emissivity	The capability of a surface to emit light comparatively to the blackbody
MODTRAN	Moderate spectral resolution software for computation of the radiative parameters of the atmosphere
ASTER	A sensor operating with five bands in the thermal infrared and a number of bands in the other spectral bands. It is on board a NASA satellite
ISSTES	Iterative spectral smoothing temperature emissivity separation.
PIXEL	Picture elements: Units of which an image is composed. In hyperspectral imagery it is generally the measured spectral radiance corresponding to an element of the surface of the ground

Distribution list

INTERNAL

DRDC-Valcartier TM 2004-123

1- Director General
3- Document Library
1- Pierre Lahaie (author)
1- Hd/SpO
1- Hd/EOW
1- Hd/DASO
1- J-P. Ardouin
1- M. Lévesque
1- J. Lévesque
1- D. Lavigne
1- V. Roy
1- S. Buteau
1- F. Leduc
1- A. Jouan
1- D. St-Germain
1- J-M. Thériault
1- G. Fournier
1- G. Potvin

EXTERNAL DISTRIBUTION

DRDC-Valcartier TM 2004-123

1- DRDKIM (PDF File)
1- DRDC
1- DRDC Ottawa
1- DRDC Atlantic
1- DRDC Suffield
1- DRDC Toronto
1- Director Science and technology (Command, Control, Communications, Computers, Intelligence, Surveillance, Reconnaissance (C4ISR))
1- Director Science and Technology (Land)
1- Director Science and Technology (Policy)
1- Director Science and Technology (Maritime)
1- Director Science and Technology (Air)
1- Director Science and Technology (Human Performance)
1- J2 DSI (Directorate Strategic Information)

1- Lcol. Yvan Choiniere
DSPaceD
National Defence Headquarters
101 Colonel By Drive
Ottawa, Ontario, K1A 0K2

1- Capt John Klatt
National Defence Headquarters
101 Colonel By Drive
Ottawa, Ontario, K1A 0K2

1- Chuck Livingstone
DRDC-Ottawa
3701 Carling Avenue
Ottawa, Ontario, K1A 0Z4

DOCUMENT CONTROL DATA

1. ORIGINATOR (name and address)	2. SECURITY CLASSIFICATION (Including special warning terms if applicable)
DRDC-Valcartier 2459, Pie-Xl blvd. North Val-Bélair, Québec G3J 1X5 Canada	Unclassified

3. TITLE (Its classification should be indicated by the appropriate abbreviation (S, C, R or U)

A new technique for separation of temperature and emissivity

4. AUTHORS (Last name, first name, middle initial. If military, show rank, e.g. Doe, Maj. John E.)

Lahaie, Pierre

5. DATE OF PUBLICATION (month and year)	6a. NO. OF PAGES	6b .NO. OF REFERENCES
December 2004	33	7

7. DESCRIPTIVE NOTES (the category of the document, e.g. technical report, technical note or memorandum. Give the inclusive dates when a specific reporting period is covered.)

Technical memorandum

8. SPONSORING ACTIVITY (name and address)

DRDC

9a. PROJECT OR GRANT NO. (Please specify whether project or grant)	9b. CONTRACT NO.
WBE 15ev11	

10a. ORIGINATOR'S DOCUMENT NUMBER	10b. OTHER DOCUMENT NOS
TM 2004-124	N/A

11. DOCUMENT AVAILABILITY (any limitations on further dissemination of the document, other than those imposed by security classification)

- ☒ Unlimited distribution
- ☐ Restricted to contractors in approved countries (specify)
- ☐ Restricted to Canadian contractors (with need-to-know)
- ☐ Restricted to Government (with need-to-know)
- ☐ Restricted to Defense departments
- ☐ Others

12. DOCUMENT ANNOUNCEMENT (any limitation to the bibliographic announcement of this document. This will normally correspond to the Document Availability (11). However, where further distribution (beyond the audience specified in 11) is possible, a wider announcement audience may be selected.)

13. ABSTRACT (a brief and factual summary of the document. It may also appear elsewhere in the body of the document itself. It is highly desirable that the abstract of classified documents be unclassified. Each paragraph of the abstract shall begin with an indication of the security classification of the information in the paragraph (unless the document itself is unclassified) represented as (S), (C), (R), or (U). It is not necessary to include here abstracts in both official languages unless the text is bilingual).

We describe in this report a new technique for the separation of temperature and emissivity in the thermal infrared part of the electromagnetic spectrum. The measurement taken with by a passive remote sensing instrument is radiance. This radiance is a combination of components originating from the atmosphere and from the ground. Once the atmospheric contribution is removed, the result is radiance from the ground that depends on its fundamental parameters i.e. temperature and emissivity. These parameters are useful to determine the nature and use of the material under observation. The new technique presented here is based on an iterative scheme for the selection of temperature and of its corresponding emissivity. At each temperature it evaluates a criterion, the total square error. The selected temperature is the one showing the smallest error. To evaluate the error we first compute the equivalent emissivity at a given temperature, we smooth the emissivity using a linear procedure then we compute a new radiance for the smoothed emissivity. The error is computed by the summation of the squared difference between the ground radiance and the new radiance. This technique is robust to noise and atmospheric parameters errors. The currently airborne imaging FTIR sensor (AIRIS) built by DRDC Valcartier is targeted as an application of interest for this algorithm. However, it can be applied to imaging sensor with at least six bands.

14. KEYWORDS, DESCRIPTORS or IDENTIFIERS (technically meaningful terms or short phrases that characterize a document and could be helpful in cataloguing the document. They should be selected so that no security classification is required. Identifiers, such as equipment model designation, trade name, military project code name, geographic location may also be included. If possible keywords should be selected from a published thesaurus, e.g. Thesaurus of Engineering and Scientific Terms (TEST) and that thesaurus-identified. If it is not possible to select indexing terms which are Unclassified, the classification of each should be indicated as with the title.)

Emissivity, Temperature, Thermal hyperspectral imagery, Atmospheric correction,

Defence R&D Canada

Canada's leader in defence
and national security R&D

R & D pour la défense Canada

Chef de file au Canada en R & D
pour la défense et la sécurité nationale

WWW.drdc-rddc.gc.ca